

# PHOTODIODE CALIBRATION USING AN ELECTRICAL SUBSTITUTION RADIOMETER IN THE HARD X-RAY REGION\*

N.I. Bolibruch, J.M. Vogt, R. Igarashi, Canadian Light Source, Saskatoon, SK, Canada

## Abstract

An electrical substitution radiometer under development at the Canadian Light Source (CLS) has been used to calibrate a photodiode (AXUV100) from International Radiation Detectors Inc. within an energy range of 8 keV to 30 keV. These measurements were made using monochromatic X-rays on the Biomedical Imaging and Therapy bend magnet beamline and the Hard X-Ray Microanalysis beamline at the CLS. The results were then compared with silicon absorption calculations using data from the NIST mass absorption coefficient tables. Good agreement has been found between the diode calibration obtained from the radiometer and the theoretical calculation of the diode response.

## INTRODUCTION

Electrical Substitution Radiometers (ESR) are used as a radiometric standard for radiation measurement at many national standards institutes around the world [1][2][3][4]. Considering ESR is a well-established method of power measurement, the CLS is developing an electrical substitution radiometer to calibrate detectors used within the facility and for use during the commissioning of beamlines.

In this paper we will overview the design, development, performance characteristics and initial measurements taken with the radiometer. Much of the design process was focused on the development of the radiation absorber, particularly thermal and X-ray interactions. A heat transfer model was developed in MATLAB, and is used as the basis for new absorber design. To determine secondary power losses, X-ray particle interactions were modelled using a Monte-Carlo particle physics simulation package named FLUKA [5]. After the radiometer was constructed, thermal tests were conducted to determine the measurement sensitivity and time response. These measurements were then followed with monochromatic power measurements taken at the Hard X-ray microanalysis beamline (HXMA) [6], as well as the Biomedical Imaging and Therapy bend magnet beamline (BMIT-BM) [7].

## RADIOMETER DESIGN

The design process of the radiometer consisted of five stages: cryostat design, temperature control system design, thermal modelling, alignment system design, and Monte-Carlo particle simulation.

## Cryostat Design

The radiometer was built by the Janis Research Company onto their Model 8CNDT liquid helium cryostat. The cryostat has a sample chamber with a beryllium window, and a liquid nitrogen cooled baffle, as seen in Figure 1. A secondary snout located further in the radiometer is connected to the liquid helium cooled portion of the cryostat, and has a small piece of aluminized Mylar covering the opening to shield the absorber from infrared. The radiation absorber used is suspended with wires in the centre of the radiometer sample chamber, and is composed of gold plated copper foil rolled into a cone, as seen in Figure 2. A second identical sample chamber, without the cryostat was also supplied by Janis, and is used to house the detector that is calibrated against the radiometer.

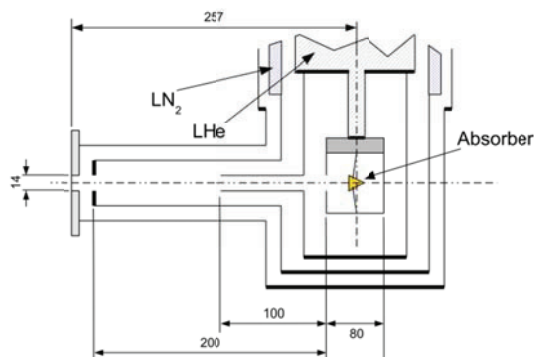


Figure 1: Diagram of the Absorber chamber of the radiometer used at Canadian Light Source. (Not to scale)

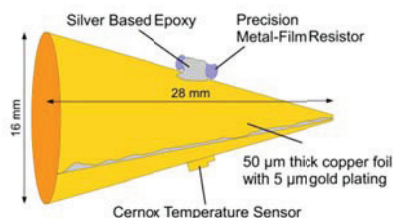


Figure 2: Radiation absorber with temperature sensor and heating resistor.

## Temperature Control System

The radiometer operates under the principle of electrical substitution. Using a PID controller, a constant absorber temperature can be maintained by adjusting power applied to a heating resistor attached to the radiation absorber. By measuring the difference in power between the beam off and beam on state, the amount of power provided by the radiation source can be determined. The temperature control system used for the radiometer

\*Work supported by NSERC, NRC, CIHR, WEDC.

consists of three major components: resistor power dissipation measurement, DC current source, and temperature measurement, shown in Figure 3.

To measure the power dissipation of the heating resistor, low noise, high precision electronics are necessary. The current and voltage measured across the heating resistor are taken with Keithley 2000MM Multimeters, and a Keithley 6220 DC Current Source is used to supply current. Temperature measurements on the absorber were made using a Cernox CX-1050 temperature sensor manufactured by Lakeshore Cryotronics, and measured on a Lakeshore 211 Temperature Monitor.

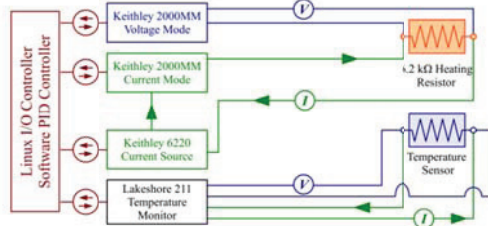


Figure 3: Temperature control system used to maintain constant temperature on the radiometer absorber.

### Thermal Model

A thermal model was created in MATLAB to approximate the behaviour of an absorber. Important characteristics for the absorber were its response time and thermal sensitivity. This needed to be in balance with the overall mass of the absorber, as X-ray absorption is highly dependent on material thickness.

The thermal model takes into consideration multiple heat sources. Blackbody IR emitted by the room temperature beryllium window, heat dissipated by the temperature sensor, and the radiation source to be measured. Heat is carried away from the absorber in multiple ways: The heat is conducted via 12, 0.14 mm diameter Phosphor-Bronze wires and a 0.115 mm copper wire. These wires are heat sunk against a metal frame in which the absorber resides. Energy is also lost via radiative processes since the absorber will be at a temperature higher than the surrounding environment. A steady state is ultimately reached between the gains and losses, which is simulated in MATLAB and compared to observed temperature change shown in Figure 4.

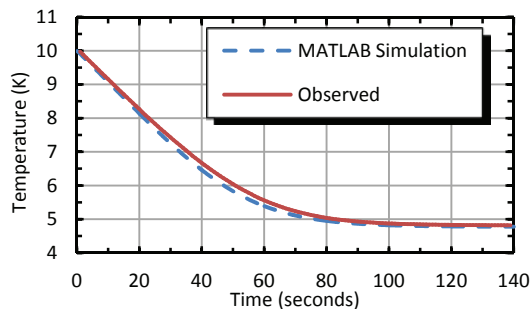


Figure 4: Comparison of MATLAB simulation and observed absorber temperature change.

### Monte-Carlo Simulation

A final part in the design process of the absorber was several Monte-Carlo particle simulations conducted using the FLUKA particle interaction software package. FLUKA can transport photons as low as 100 eV at the time of writing, however for the simulations used; only photons above 1 keV were considered, as many properties of lower energy photons are not handled without considerable code customization. The simulations were conducted to optimize the materials and absorber geometry for X-ray absorption between 8 keV and 30 keV, in addition to any beam misalignment, with beam offsets up to 5 mm.

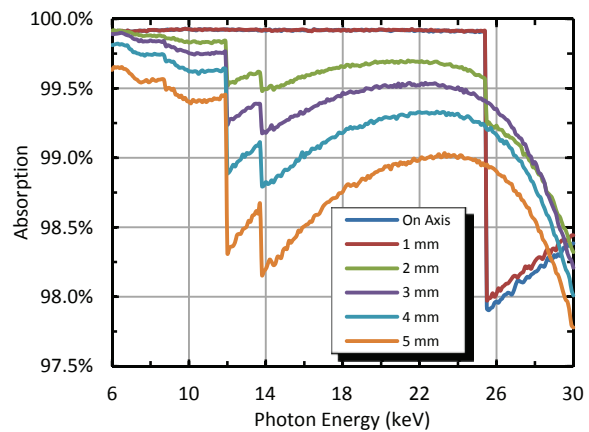


Figure 5: Monte-Carlo simulation of absorption dependence on beam misalignment. The beam used is a Gaussian shape with a FWHM of 0.75 mm in both X and Y.

### Alignment System

Since the radiometer is a mobile system and will be used at multiple beamlines, the radiometer required a system of alignment. As shown in the Monte-Carlo simulations (Figure 5), beam misalignment may reduce absorption to 98%. A dismountable alignment system designed similarly to a Michelson Interferometer was built. The alignment system is mounted to the frame of the radiometer, and is aligned to the absorber, with an anti-reflection window substituting the beryllium window, during a prior cool-down session.

### RADIOMETER MEASUREMENTS

Measurements to calibrate the photodiode were conducted for energies of 8 and 10 keV at the HXMA beamline, while measurements for 15 to 30 keV were made at the BMIT-BM beamline. Shown in Table 1 are the relative uncertainties for the measurements taken, determined for the corresponding photon energy measurements. The alignment uncertainty is based on the results of the FLUKA Monte-Carlo simulation, as the percentage of absorption varies based on the alignment of the beam. The alignment uncertainty considers worst case alignment error of up to 5 mm. The photocurrent uncertainty due to noise is clearly the largest contributor across all the measurements, except for the 15 keV

measurements. The systematic uncertainty of the photocurrent measurement is estimated to be less than 100 ppm. The radiometer power uncertainty is determined from obtaining a large sample of power measurements while the radiometer absorber temperature was placed at a specific set point. The systematic uncertainty of the power measurement is estimated to be less than 100 ppm, and considered negligible.

Table 1: Relative Uncertainty in AXUV100 Diode Response (A/W) Measurement  $\times 100$

Photon Energy (keV)	Alignment Uncertainty	Photodiode Current Uncertainty	Radiometer Power Uncertainty	Total Relative Uncertainty
8	0.2610	3.5080	0.2661	3.5277
10	0.3677	3.5080	0.0759	3.5280
15	1.1213	1.0659	0.2661	1.5698
18	0.8299	1.0292	0.2425	1.3442
20	0.7177	3.1418	0.3656	3.2434
22	0.6610	1.5250	0.2425	1.6797
24	0.6524	2.0228	0.2425	2.1392
26	0.6741	2.6453	0.2425	2.7406
28	0.2686	3.8409	0.2543	3.8587
30	0.4367	7.3094	0.2661	7.3272

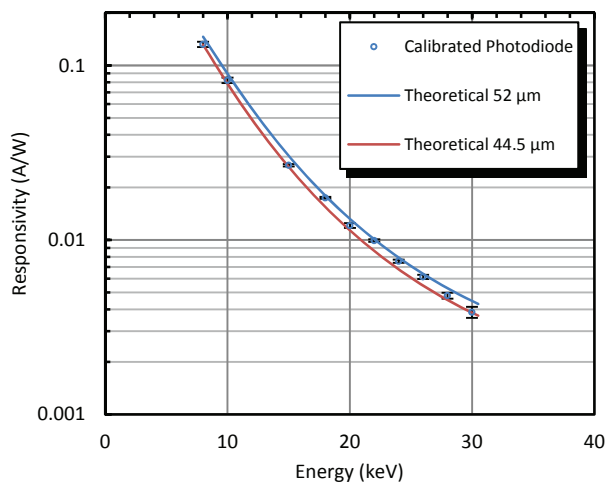


Figure 6: Responsivity of the AXUV100 photodiode as determined by the Radiometer and compared to photon absorption models for 44.5 and 52  $\mu\text{m}$  of silicon.

In Figure 6, the responsivity of the AXUV100 photodiode is plotted against the theoretical responsivity as determined by photon absorption of 44.5 and 52  $\mu\text{m}$  of silicon. These thicknesses were chosen as they encompass all of the data points. Considering the AXUV100 photodiode is not bare silicon, but is attached

to a Steatite package using a metal based epoxy, the responsivity will not strictly follow the silicon absorption model, particularly at higher energies, as the metal based epoxy will create fluorescence photons. The silicon thickness is also variable between regions, and could introduce considerable variation between measurements if the diode was repositioned.

## CONCLUSIONS

Comparing the theoretical responsivity of an AXUV100 photodiode and the CLS developed electrical substitution radiometer derived responsivity show good agreement with the theoretical responsivity of silicon over an energy range of 8 keV and 30 keV. Steps will be taken to reduce photocurrent, alignment, and power measurement uncertainty in future measurements. Results from a calibration of the same diode to be conducted at Physikalisch-Technische Bundesanstalt using the SYRES II radiometer will aid in validating any future results.

## REFERENCES

- [1] T. R. Gentile, J. M. Houston, J. E. Hardis, C. L. Cromer, and A. C. Parr, "National Institute of Standards and Technology high-accuracy cryogenic radiometer", *Appl. Opt.* 35, 1056-1068 (1996)
- [2] H. Rabus, V. Persch, and G. Ulm, "Synchrotron-radiation-operated cryogenic electrical-substitution radiometer as the high-accuracy primary detector standard in the ultraviolet, vacuum-ultraviolet, and soft-x-ray spectral ranges", *Appl. Opt.* 36, 5421-5440 (1997)
- [3] L.P. Boivin and K. Gibb, "Monochromator-based cryogenic radiometry at the NRC", *Metrologia*, 32, 565 (1995)
- [4] M Gerlach, M Krumrey, L Cibik, P Müller, H Rabus and G Ulm, "Cryogenic radiometry in the hard x-ray range", *Metrologia* 45, 577 (2008)
- [5] G. Battistoni, S. Muraro, P.R. Sala, F. Cerutti, A. Ferrari, S. Roesler, A. Fasso', and J. Ranft, "The FLUKA code: Description and benchmarking", *AIP Conference Proceeding* 896, 31-49, (2007)
- [6] D. T. Jiang, N. Chen, L. Zhang, K. Malgorzata, G. Wright, R. Igarashi, D. Beauregard, M. Kirkham, and M. McKibben, "XAFS at the Canadian Light Source", *AIP Conf. Proc.* 882, 893 (2007)
- [7] T.W. Wysokinski, D. Chapman, G. Adams, M. Renier, P. Suortti, and W. Thomlinson, "Beamlines of the biomedical imaging and therapy facility at the Canadian light source--Part 1", *Nucl. Instr. Meth. Phys. Res. A.* 582, 1,73-76 (2007)